

Solution to the Thomson problem for Clifford tori with an application to Wigner crystals

Amer Alrakik,[†] Miguel Escobar Azor,^{†,‡,¶} Véronique Brumas,[†] Gian Luigi
Bendazzoli,[§] Stefano Evangelisti,^{*,†} and J. Arjan Berger^{*,†,¶}

[†]*Laboratoire de Chimie et Physique Quantiques, CNRS, Université de Toulouse 3 Paul
Sabatier, 118 route de Narbonne, Toulouse, 31062 France*

[‡]*Department of Physics, University of Warwick, Coventry CV4 7AL, United Kingdom*

[¶]*European Theoretical Spectroscopy Facility (ETSF)*

[§]*Università di Bologna, Via Irnerio 33, 40126 Bologna, Italy*

E-mail: stefano.evangelisti@irsamc.ups-tlse.fr; arjan.berger@irsamc.ups-tlse.fr

Abstract

In its original version, the Thomson problem consists of the search for the minimum-energy configuration of a set of point-like electrons that are confined to the surface of a two-dimensional sphere (\mathcal{S}^2) that repel each other according to Coulomb's law, in which the distance is the Euclidean distance in the embedding space of the sphere, *i.e.*, \mathbb{R}^3 . In this work, we consider the analogous problem where the electrons are confined to an n -dimensional flat Clifford torus \mathcal{T}^n with $n = 1, 2, 3$. Since the torus \mathcal{T}^n can be embedded in the complex manifold \mathbb{C}^n , we define the distance in the Coulomb law as the Euclidean distance in \mathbb{C}^n , in analogy to what is done for the Thomson problem on the sphere. The Thomson problem on a Clifford torus is of interest because super-cells with the topology of Clifford torus can be used to describe periodic systems such as Wigner crystals. In this work we numerically solve the Thomson problem on a square

Clifford torus. To illustrate the usefulness of our approach we apply it to Wigner crystals. We demonstrate that the equilibrium configurations we obtain for a large numbers of electrons are consistent with the predicted structures of Wigner crystals. Finally, in the one-dimensional case we analytically obtain the energy spectrum and the phonon dispersion law.

1 Introduction

In 1904, Joseph John Thomson, the discoverer of the electron, proposed a model for the atomic structure that later became known as the plum-pudding model¹. In this scheme, the electrons are treated as point-like charges embedded in a large, positively charged spherical nucleus. This description soon turned out to be incorrect and was quickly abandoned and replaced by the Rutherford's solar-system model. Today, the plum-pudding model has essentially just a historical interest. This approach, however, gave rise to a very prolific mathematical literature, centered on the so-called Thomson problem. This problem aims to find the minimum-energy configuration of N point-like electrons that are confined to the surface of a two-dimensional sphere and subject to the repulsive force described by Coulomb's law. For a small number of electrons the exact solution to this problem is sometimes known, even though in some cases the proof is far from trivial². Numerical solutions, instead, are available up to very large values of N (several hundreds). We note that the original Thomson problem has been generalized to a wide class of potentials and to a various number of spatial dimensions^{3–15}.

In chemistry, the Thomson problem has found a direct application in the valence-shell electron-pair repulsion (VSEPR) theory of Gillespie and Nyholm, which permits to predict the local shape of a molecule by minimizing the Coulomb repulsion energy of negatively charged electron pairs that surround a positively charged nucleus¹⁶. The VSEPR formalism concerns a small number of electron pairs only, from 2 pairs, *e.g.* BeH_2 , up to at most 9 pairs, *e.g.* ReH_9^{2-} in the K_2ReH_9 ionic crystal. In physics and chemistry, applications of the

Thomson problem to a large numbers of electrons have been relatively rare up to now.

In a series of recent papers^{17–20} we have shown that periodic, n -dimensional crystalline systems can be conveniently mapped onto a Clifford torus \mathcal{T}^n . One of the reasons for the success of this approach is that Clifford tori are flat manifolds, which means that a fragment of a crystal can be modified to the topology of a Clifford torus without deformation. We note that, on the contrary, a similar statement is, in general, not true for spheres, *i.e.*, a fragment of a crystal *cannot* be modified to the topology of a sphere without deformation. For this reason, mapping super-cells onto spheres is not a particularly useful model for two- and three-dimensional crystals. An interesting application of our approach is the mapping of Wigner crystals on a Clifford torus. A Wigner crystal is a crystalline structure that forms in a system of interacting electrons at sufficiently low density, in which the electrons localize at periodic lattice sites. This concept was first proposed by Eugene Wigner in 1934, who predicted that in a neutralizing uniform background, the repulsive interactions between electrons would dominate over the kinetic energy of the electrons at low densities.^{21,22} This would result in the formation of a crystalline structure where the electrons occupy the lattice sites, leading to a decrease in the potential energy of the system. A two-dimensional Wigner crystal has recently been observed experimentally by Smolenski and coworkers²³. Two-dimensional crystal lattices made up of electrons have also been obtained experimentally on the surface of liquid Helium²⁴, in magnetic fields^{25–31} and in Moiré superlattices^{32–35}. Such systems are often also referred to as Wigner crystals in the literature. Wigner crystals have also been observed in one dimension^{36–38}. The properties of Wigner crystals have been studied extensively in condensed matter physics and have important implications for the understanding of the behavior of electrons in low-dimensional systems. Closely related to Wigner crystals are Wigner molecules, which are confined few-electron systems in which the electrons form a stable bound state due to their mutual repulsion^{20,39–48}. Experimental observations of Wigner molecules have been reported in various physical systems, including carbon nanotubes⁴⁹, nanowires^{50,51} and in quantum dots⁵².

In our previous works, we have shown that a set of point-like electrons placed on Clifford tori \mathcal{T}^n of different dimensions ($n=1,2,3$) can efficiently represent a fragment of a classical Wigner crystal^{19,20,48}. In particular, we have been able to compute the classical electrostatic energies as well as the harmonic corrections of Wigner crystals with unprecedented precision¹⁹. This precision has been attained thanks to an extrapolation of the results obtained for finite systems. An advantage of calculations performed using Clifford periodic boundary conditions, and contrary to calculations performed within open-boundary conditions, is that there are no border effects which hamper the extrapolation of the results obtained for finite systems to the thermodynamic limit. One of the main issues in the study of Wigner crystals remains the prediction of the energy and stability of the different possible space groups that the system can adopt and, in particular, the prediction of the space group that corresponds to the ground state. Usually the ground-state configuration is obtained by comparing the energies of only a few well-known space groups. However, this leaves open the possibility that a less trivial configuration has a lower energy. In this paper, we tackle this problem by generalizing the Thomson problem to Clifford tori. We will show that this approach permits us to predict the geometrical structure of Wigner crystals.

This article is organized as follows. In section 2, we give the details of the Thomson problem on Clifford tori. We give the computational details of our numerical approach in section 3. In section 4, we report and discuss some results we obtain with our approach. We will focus on Clifford tori that contain numbers of electrons that are compatible with Wigner crystals. We discuss the analytical treatment of the one-dimensional case in section 5. Finally, in Section 6 we draw the conclusions of our work and briefly discuss how our approach can be generalized to perform periodic molecular mechanics simulations.

2 The Thomson Problem on a Clifford torus

The original Thomson problem pertains to point-like electrons that are confined to the surface of a two-dimensional sphere and that repel each other according to Coulomb's law and the goal is to find the configuration of the electrons that corresponds to the lowest energy. The distance in the Coulomb interaction is defined as the Euclidean distance in the embedding space of the sphere, *i.e.*, \mathbb{R}^3 . Here we consider the analogous problem where the electrons are confined to an n -dimensional (nD) Clifford torus \mathcal{T}^n with $n = 1, 2, 3$. A Clifford torus is obtained by joining the opposite points of a line (1D), the opposite edges of a rectangle (2D), or the opposite faces of a cuboid (3D), without deformation. Analogous to the original problem, we define the distance in the Coulomb potential as the Euclidean distance in the embedding space of the Clifford torus, *i.e.*, \mathbb{C}^n . This distance d_{ij} between electrons i and j is thus defined as^{17–20,53}

$$d_{ij} = \sqrt{\sum_{\alpha=1}^n \left[\frac{L_{\alpha}}{\pi} \sin \left(\frac{\pi}{L_{\alpha}} [x_{\alpha,i} - x_{\alpha,j}] \right) \right]^2}, \quad (1)$$

where L_{α} is the length of an edge along the α -direction of the Clifford torus. The Coulomb potential U is given by (in Hartree atomic units)

$$U = \frac{1}{2} \sum_{i=1}^N \sum_{\substack{j=1 \\ j \neq i}}^N d_{ij}^{-1}, \quad (2)$$

with d_{ij} given in Eq. (1). The Thomson problem on a Clifford torus consists of minimizing the corresponding Coulomb energy with respect to the positions of the electrons on the Clifford torus. In order to guarantee that a minimum is obtained the gradient of U has to vanish and all the eigenvalues of the Hessian of U should be non-negative while exactly n eigenvalues should be equal to zero. They correspond to the n translational degrees of freedom in the Clifford torus. Furthermore, there are $n(n-1)/2$ eigenvalues that asymptotically vanish when L tends to infinity for a fixed number of electrons. They correspond to

rotational degrees of freedom. For example, in the 3D case, there are three eigenvalues that are identically zero corresponding to the translations, and three asymptotically vanishing eigenvalues corresponding to the rotations. Finally, we note that the Thomson problem in one dimension is equivalent to the well-known Thomson problem on a circle of radius R and length $L = 2\pi R$. The minimum-energy configuration on the circle is obtained by placing the N electrons on the vertices of a regular polygon with n sides. On the 1D Clifford torus this corresponds to the positions of the electrons being equidistant. A complete analytical treatment of the 1D case is presented in section 5.

In two and three dimensions we can, in principle, solve the Thomson problem numerically for any number of electrons with our approach. For a large number of electrons we expect that the positions of the electrons correspond to the lattices of Wigner crystals, i.e., a hexagonal (or triangular) lattice in two dimensions and a body-centred cubic lattice in three dimensions^{19,54,55}.

3 Computational Details

We wrote a computer code to numerically solve the Thomson problem on a Clifford torus in one, two, and three dimensions. It uses the analytical expressions of the gradient and the Hessian of the Coulomb potential in Eq. 2. These expressions are reported in appendix A. We note that our code could be easily generalized to higher dimensions but this is beyond the scope of our investigation. The program uses the conjugated gradient algorithm to minimize the Coulomb energy on the Clifford torus. We use a total gradient-norm tolerance of 10^{-14} Hartree. We verified that, at convergence, the eigenvalues of the Hessian of the Coulomb potential are all positive except for n zero eigenvalues that correspond to the translational degrees of freedom. To ensure that we find the global minimum and not a local minimum we have performed several calculations for a given Thomson problem starting from different initial positions of the electrons. In practice, our code allows us to solve the

Thomson problem numerically up to several thousands of electrons.

Our code can also be used to obtain information about structures that do not correspond to the global minimum of the potential energy surface by fixing the electrons to certain positions, e.g., those corresponding to a known crystal lattice. After verifying that the gradient of U vanishes, we can then learn from the Hessian whether this structure corresponds to a stationary point and, if this is the case, what is the nature of the stationary point (a minimum or a saddle point). In the following, whenever the Hessian is analysed for a given configuration of electrons, it is implied that the gradient of U vanishes for this configuration. Finally, we note that the code with which all results in this work were obtained is freely available⁵⁶.

4 Results

In this section we present the numerical solutions we have obtained for the Thomson problem on a Clifford torus. We will focus here on two and three dimensions since the analytical result for one dimension is given in section 5. We note that we have verified that our numerical results in one dimension are consistent with the analytical results. Although our method can be applied to the Thomson problem on a Clifford torus for any number of electrons, we focus here on a relatively large number of electrons ($N \sim 100$) since we want to observe the lattice structures of Wigner crystals. Finally, all the numerical solutions we present in this section, i.e., the positions of the electrons, can be found in Ref. [56].

4.1 2-dimensional Clifford tori

Although Eq. (2) depends on the lengths of the two edges of the Clifford torus, L_x and L_y , the relative positions corresponding to the solution of the Thomson problem only depend on the ratio $r = L_y/L_x$. Therefore, in the following we will only refer to r and N when discussing the solutions to the Thomson problem in 2D. In Fig. 1 we report the solution

of the Thomson problem for $r = 1$ and $N = 120$. Even though $r = 1$ is not compatible with a hexagonal lattice, we clearly observe a hexagonal lattice with a small distortion. The

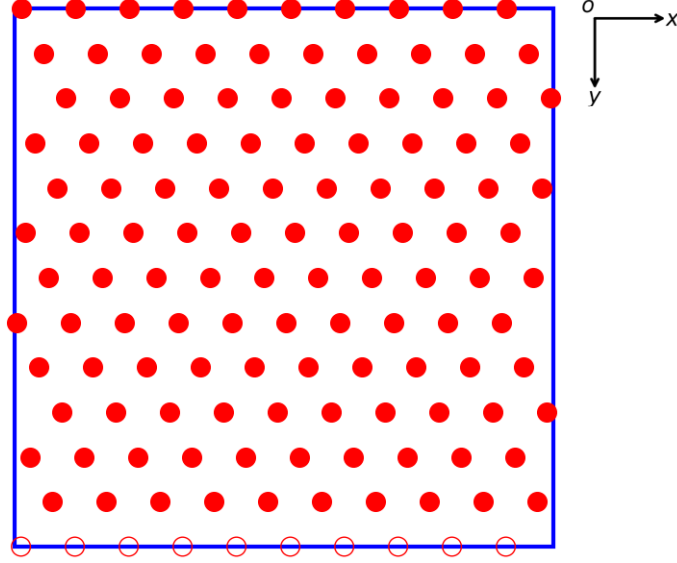


Figure 1: The solution to the Thomson problem for 120 electrons on a square Clifford torus ($r = 1$). Filled circles: the positions of the electrons; open circles: the equivalent positions of the electrons on the edge of the Clifford torus.

hexagonal lattice is commensurable with the Clifford torus when $r = \sqrt{3}/2$ and $N = 4m^2$ with m a positive integer. In Fig. 2 we report the solution to the Thomson problem on a Clifford torus with 100 electrons ($m = 5$) and $r = \sqrt{3}/2$. We now observe a perfect hexagonal lattice. In general, we find that for $r = \sqrt{3}/2$ and $N = 4m^2$ the solution to the Thomson problem is a hexagonal lattice for $m > 1$. Finally, we note that there are other combinations of r and N that are commensurable with the hexagonal lattice, e.g., $r = \sqrt{3}$ and $N = 2m^2$.

With our approach we can also verify that the square lattice is not a solution to the Thomson problem on the Clifford torus by imposing a square lattice and calculating the corresponding Hessian. A square lattice is commensurable with a Clifford torus Where $r = 1$ and $N = m^2$ with m a positive integer. We have verified that the square lattice does not correspond to a minimum but to a saddle point, since the the corresponding Hessian has negative eigenvalues. Our results are consistent with the prediction that the lattice structure of the two-dimensional Wigner crystal is the hexagonal lattice. As mentioned before, this

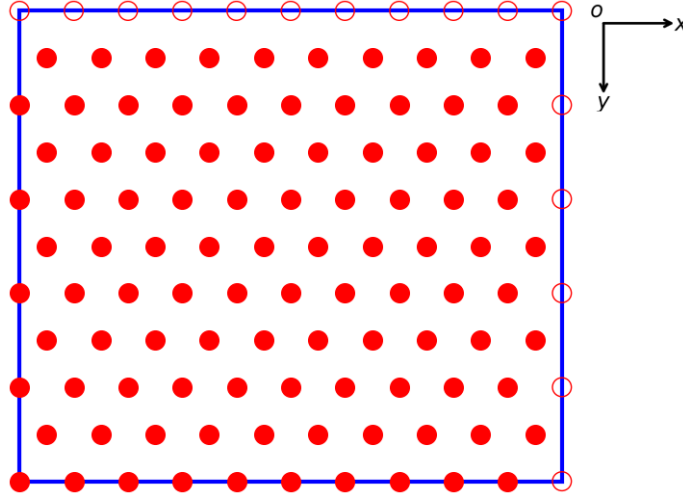


Figure 2: The solution to the Thomson problem for 100 electrons on a Clifford torus ($r = \sqrt{3}/2$). Filled circles: the positions of the electrons; open circles: the equivalent positions of the electrons on the edge of the Clifford torus. The positions of the electrons correspond to a hexagonal lattice.

prediction is based on the comparison of the ground-state energy of the hexagonal lattice with other known lattices and, in particular, the square lattice. In our approach the hexagonal lattice emerges naturally.

4.2 3-dimensional Clifford tori

In three dimensions the relative positions of the electrons corresponding to the solution of the Thomson problem on a Clifford torus depend on the number of electrons N and on the ratios L_y/L_x and L_z/L_x . Here we will focus on cubic Clifford tori, i.e., $L_x = L_y = L_z$, with numbers of electrons that are commensurable either with the body-centred cubic (bcc) lattice, i.e., $N = 2m^3$, or with the face-centred cubic (fcc) lattice, i.e., $N = 4m^3$, with m a positive integer. We note that N can never be commensurable with both the bcc and fcc lattices. We find that the fcc lattice is the solution to the Thomson problem for 4 ($m = 1$), 32 ($m = 2$), and 108 ($m = 3$) electrons. As an example, we report in Fig. 3 the solution to the Thomson problem for a cubic Clifford torus with 32 electrons ($m = 2$). We have also verified that the fcc lattice is (at least) a local minimum for values of $4 \leq m \leq 10$ since the

corresponding Hessian matrices have no negative eigenvalues for these values of m .

Instead, for a number of electrons compatible with the bcc lattice the situation is more complicated. With only 2 electrons ($m = 1$) the solution to the Thomson problem is the bcc lattice, with one electron on a vertex and the other in the center of the cube. Instead for 16 electrons ($m = 2$) the bcc lattice is not a minimum but a saddle point. In Fig. 4 we show the solution to the Thomson problem on a cubic Clifford torus with 16 electrons. The electrons localise in planes that are parallel to the plane containing the diagonal of the cube. In Fig. 5 we show the solution to the Thomson problem on a cubic Clifford torus with 54 electrons ($m = 3$). In this case the bcc lattice corresponds to a local minimum but not to the global minimum. For 128 electrons ($m = 4$) the bcc lattice is again the solution to the Thomson problem. We report that solution in Fig. 6; we clearly see that the electrons form a body-centred cubic (bcc) lattice. Furthermore, we have verified that the bcc lattice is (at least) a local minimum for values of $5 \leq m \leq 13$ since the corresponding Hessian matrices have no negative eigenvalues for these values of m . Finally, we have also verified that the simple cubic (sc) lattice is never a solutions to the Thomson problem on a cubic Clifford torus even when the number of electrons is commensurable with the sc lattice, i.e., $N = m^3$. Indeed, we find that these structures correspond to saddle points in the potential energy surface.

5 The Thomson problem on a one-dimensional Clifford torus

In this section, we consider the analytical treatment of Thomson problem of N electrons on a 1D Clifford torus of length L . Without loss of generality, we assume that the positions x_i (modulus L) of the electrons i are given in ascending order according to

$$i < j \Rightarrow x_i < x_j \pmod{L}. \quad (3)$$

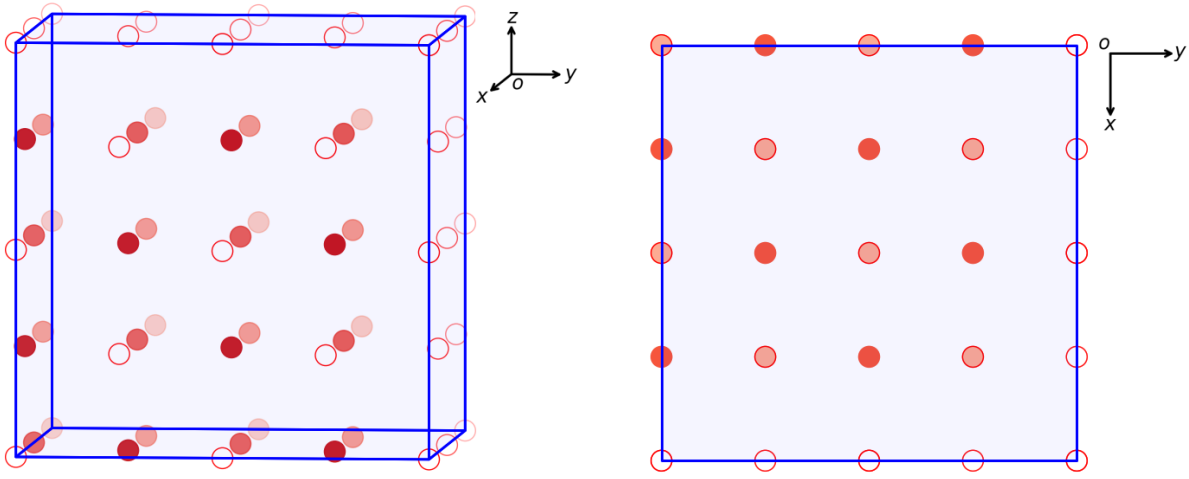


Figure 3: The solution to the Thomson problem for 32 electrons on a cubic Clifford torus. Filled circles: the positions of the electrons (lighter shades represent electrons that are deeper); open circles : the equivalent positions of the electrons on the faces of the Clifford torus. Left panel: front view; right panel: top view. The positions of the electrons correspond to an fcc lattice.

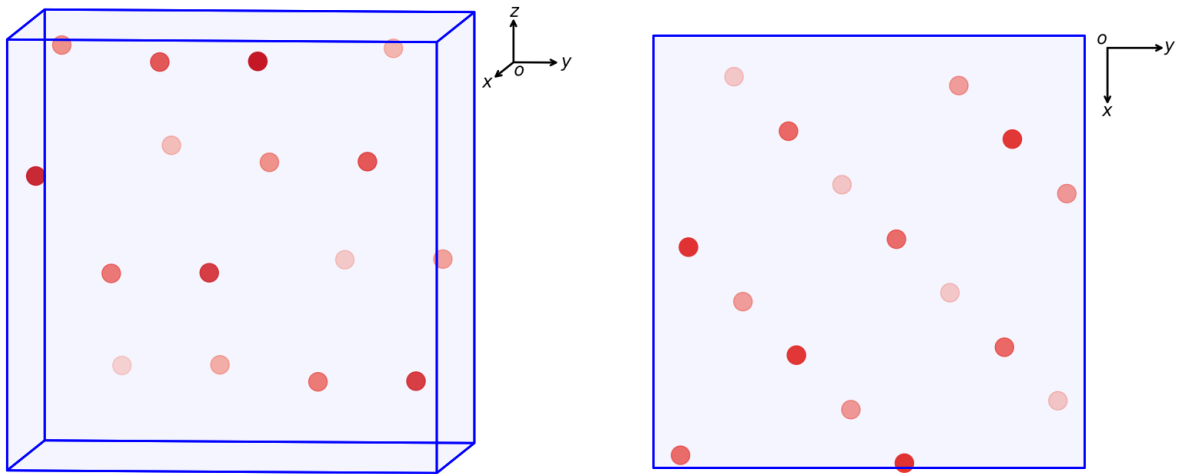


Figure 4: The solution to the Thomson problem for 16 electrons on a cubic Clifford torus. Filled circles: the positions of the electrons (lighter shades represent electrons that are deeper);. Left panel: front view; right panel: top view.

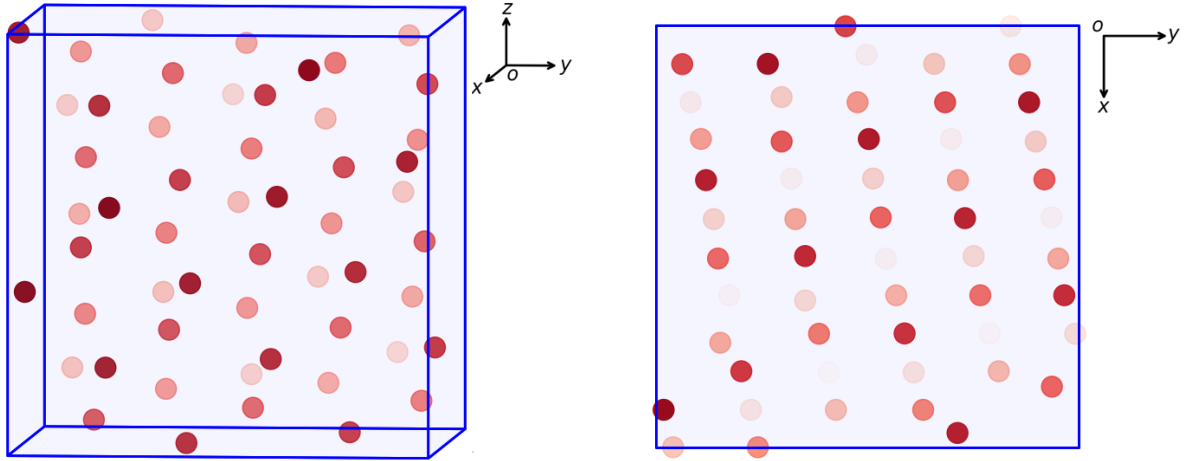


Figure 5: The solution to the Thomson problem for 54 electrons on a cubic Clifford torus. Filled circles: the positions of the electrons (lighter shades represent electrons that are deeper). Left panel: front view; right panel: top view.

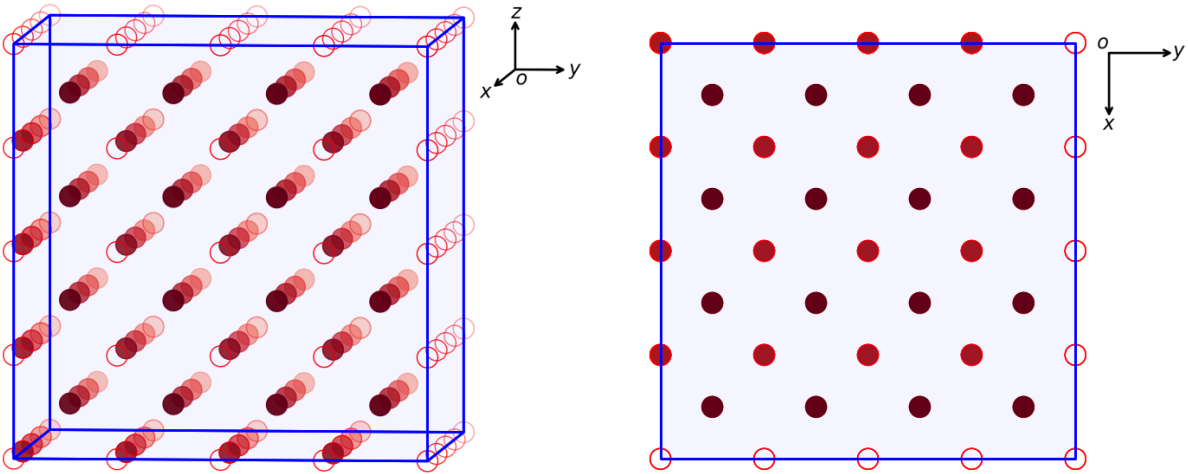


Figure 6: The solution to the Thomson problem for 128 electrons on a cubic Clifford torus. Filled circles: the positions of the electrons (lighter shades represent electrons that are deeper); open circles: the equivalent positions of the electrons on the faces of the Clifford torus. Left panel: front view; right panel: top view. The positions of the electrons correspond to a bcc lattice.

In 1D we can write the total energy U as

$$U = \frac{1}{2} \frac{\pi}{L} \sum_{i=1}^N \sum_{\substack{j=1 \\ j \neq i}}^N \sin \left[\frac{\pi}{L} |x_i - x_j| \right]^{-1}. \quad (4)$$

It can be verified that this expression is equal to Eq. (2) for values of x_i (and x_j) on the Clifford torus to which the electrons are confined, i.e., $0 \leq x_i \leq L$.

We now show that the equally spaced arrangement of N electrons on the 1D Clifford torus is a stationary point in the one-dimensional energy surface. The gradient of the potential energy has the following components

$$g_k = \frac{\partial U}{\partial x_k} = \left(\frac{\pi}{L} \right)^2 \sum_{\substack{j=1 \\ j \neq k}}^N \frac{\cos \left[\frac{\pi}{L} (x_k - x_j) \right]}{\sin^2 \left[\frac{\pi}{L} |x_k - x_j| \right]} \text{sgn}(x_k - x_j). \quad (5)$$

Each term of the sum in the above equation is an odd function of the argument $x_k - x_j$. Therefore, if the electrons are equally spaced, for each value $x_k - x_j$ there will be a symmetrical value $x_k - x_{j'} = -(x_k - x_j)$, and the two corresponding contribution cancel. If the sum contains an odd number of terms there will be one contribution that will not be canceled. However, this contribution corresponds to $x_k - x_j = L/2$ which vanishes by itself. As a result, in the case of equally spaced electrons, each component g_k vanishes, and this configuration necessarily corresponds to a stationary point.

We now demonstrate that this stationary point is a minimum. This means that all the eigenvalues of the Hessian are positive with the exception of one vanishing eigenvalue that corresponds to the translation of all the electrons. The matrix elements $\mathcal{H}_{k,l}$ of the Hessian

are given by

$$\mathcal{H}_{k,k} = \frac{\partial^2 U}{\partial x_k^2} = \left(\frac{\pi}{L}\right)^3 \sum_{\substack{j=1 \\ j \neq k}}^N \frac{1 + \cos^2 \left[\frac{\pi}{L}(x_k - x_j) \right]}{\sin^3 \left[\frac{\pi}{L}|x_k - x_j| \right]}, \quad (6)$$

$$\mathcal{H}_{k,l} = \frac{\partial^2 U}{\partial x_k \partial x_l} = - \left(\frac{\pi}{L}\right)^3 \frac{1 + \cos^2 \left[\frac{\pi}{L}(x_k - x_l) \right]}{\sin^3 \left[\frac{\pi}{L}|x_k - x_l| \right]} \quad (k \neq l). \quad (7)$$

We see that the Hessian is real and symmetric. All its diagonal elements are positive while all off-diagonal elements are negative. Since all electrons are equivalent when they are equally spaced on a Clifford torus, all diagonal elements are equal to the same value. Moreover, all off-diagonal elements with the same value for $|k - l|$ have identical values. Therefore, we can write

$$\mathcal{H}_{k,l} = H_{|k-l|}. \quad (8)$$

Finally, because of the translational symmetry of the Clifford torus we have the identity

$$H_j = H_{N-j}. \quad (9)$$

By combining the above results it follows that the Hessian can be rewritten as a symmetric circulant matrix according to

$$\mathcal{H} = \left\| \begin{array}{cccccc} H_0 & H_1 & H_2 & H_3 & \dots & H_{N-2} & H_{N-1} \\ H_{N-1} & H_0 & H_1 & H_2 & \dots & H_{N-3} & H_{N-2} \\ H_{N-2} & H_{N-1} & H_0 & H_1 & \dots & H_{N-4} & H_{N-3} \\ \dots & \dots & \dots & \dots & \dots & \dots & \dots \\ H_2 & H_3 & H_4 & H_5 & \dots & H_0 & H_1 \\ H_1 & H_2 & H_3 & H_4 & \dots & H_{N-1} & H_0 \end{array} \right\| = \left\| \begin{array}{cccccc} H_0 & H_1 & H_2 & H_3 & \dots & H_2 & H_1 \\ H_1 & H_0 & H_1 & H_2 & \dots & H_3 & H_2 \\ H_2 & H_1 & H_0 & H_1 & \dots & H_4 & H_3 \\ \dots & \dots & \dots & \dots & \dots & \dots & \dots \\ H_2 & H_3 & H_4 & H_5 & \dots & H_0 & H_1 \\ H_1 & H_2 & H_3 & H_4 & \dots & H_1 & H_0 \end{array} \right\|. \quad (10)$$

in which

$$H_0(N) = \frac{\pi^3}{d^3 N^3} \sum_{j=1}^{N-1} \frac{1 + \cos^2\left(\frac{\pi j}{N}\right)}{\sin^3\left|\frac{\pi j}{N}\right|}, \quad (11)$$

$$H_j(N) = -\frac{\pi^3}{d^3 N^3} \frac{1 + \cos^2\left(\frac{\pi j}{N}\right)}{\sin^3\left|\frac{\pi j}{N}\right|} \quad (j \neq 0), \quad (12)$$

where we used that $L = Nd$ and $(x_k - x_l) = (k - l)d$ with d the nearest-neighbor distance of the electrons. From the above equations it can be easily verified that the following sum rule holds,

$$H_0 = -\sum_{j=1}^{N-1} H_j. \quad (13)$$

Since \mathcal{H} is a symmetric circulant matrix, the normalized eigenvectors are given by

$$\phi_k(N) = \frac{1}{\sqrt{N}} \begin{pmatrix} 1 \\ e^{ik\theta} \\ e^{2ik\theta} \\ \dots \\ e^{i(N-2)k\theta} \\ e^{i(N-1)k\theta} \end{pmatrix} = \frac{1}{\sqrt{N}} \begin{pmatrix} 1 \\ e^{ik\theta} \\ e^{2ik\theta} \\ \dots \\ e^{-2ik\theta} \\ e^{-ik\theta} \end{pmatrix}, \quad (14)$$

where $k = 0, \dots, N-1$, and $\theta(N) = 2\pi/N$. It follows that the corresponding eigenvalues of \mathcal{H} are given by

$$\epsilon_k(N) = \sum_{j=0}^{N-1} \cos(kj\theta) H_j, \quad (15)$$

where we used Euler's formula. Let us first focus on $k = 0$. The corresponding eigenvalue ϵ_0 is given by

$$\epsilon_0(N) = \sum_{j=0}^{N-1} H_j = 0, \quad (16)$$

which follows from the sum rule in Eq. (13). The corresponding eigenvector $\phi_0(N)$ is given

by

$$\phi_0(N) = \frac{1}{\sqrt{N}} \begin{pmatrix} 1 \\ 1 \\ 1 \\ \dots \\ 1 \\ 1 \end{pmatrix}, \quad (17)$$

which describes a collective displacement of all the electrons in the same direction and by the same amount. This is consistent with $\epsilon_0 = 0$ since a collective displacement does not modify the total energy of the system. Let us now study the eigenvalues for $k > 0$. Since all H_j are negative for $j > 0$ we have the following inequality,

$$-\sum_{j=1}^{N-1} \cos(kj\theta) H_j < -\sum_{j=1}^{N-1} H_j = H_0, \quad (18)$$

where we used once more the sum rule in Eq. (13), it follows that

$$\epsilon_k(N) > 0 \quad (\forall k > 0). \quad (19)$$

Therefore, the ϵ_k , with $k > 0$, are all strictly positive. This concludes the proof that a one-dimensional lattice of equally spaced electrons on the Clifford torus is indeed a local minimum.

Finally, it is interesting to evaluate what happens in the thermodynamic limit $N \rightarrow \infty$. The eigenvalues become

$$\lim_{N \rightarrow \infty} \epsilon_k(N) = \lim_{N \rightarrow \infty} H_0(N) + \lim_{N \rightarrow \infty} \sum_{j=1}^{N-1} \cos(kj\theta) H_j(N) \quad (20)$$

$$= \frac{2}{d^3} \sum_{j=1}^{\infty} \frac{1 - \cos(j\kappa)}{j^3}, \quad (21)$$

where $\kappa = 2\pi k/N$ is the crystal momentum, with $0 \leq \kappa < 2\pi$, and we used

$$\lim_{N \rightarrow \infty} H_0(N) = \sum_{j=1}^{\infty} \frac{2}{d^3 j^3} \quad (22)$$

$$\lim_{N \rightarrow \infty} H_j(N) = -\frac{2}{d^3 j^3}. \quad (23)$$

The summation in the above equation can be performed analytically and the result is

$$\epsilon_\kappa = \frac{1}{d^3} \left(2\zeta(3) - (\text{Li}_3(e^{i\kappa}) + \text{Li}_3(e^{-i\kappa})) \right), \quad (24)$$

where $\zeta(z)$ is the Riemann zeta function and $\text{Li}_3(z)$ is the trilogarithm function. It can be easily verified that ϵ_κ is an even function of κ . In Fig. 7 we report the angular frequencies $\omega_\kappa = \sqrt{\epsilon_\kappa}$ as a function of the crystal momentum κ corresponding to $d = 1$ Bohr. To put into evidence its behaviour around $\kappa = 0$, we show ω_κ for $\kappa \in [-\pi, \pi]$. At first sight, the curve has a broad similarity with the typical behaviour of ω_κ as a function of κ for the case of harmonic crystals, as can be found in many textbooks. In that case the derivative $\frac{d\omega_\kappa}{d\kappa}$ tends to a finite constant value when $\kappa \rightarrow 0$. It corresponds to the speed of sound at low frequencies. Instead, the curve in Fig. 7 for the one-dimensional Wigner crystal, has an infinite slope because $\frac{d\omega_\kappa}{d\kappa}$ diverges logarithmically when $\kappa \rightarrow 0$ as can be seen from the Taylor expansion of ϵ_κ around $\kappa = 0$ given by

$$\epsilon_\kappa = \frac{1}{d^3} \left[\left(\frac{3}{2} - \ln |\kappa| \right) \kappa^2 + \frac{\kappa^4}{144} + \frac{\kappa^6}{43\,200} + \frac{\kappa^8}{5\,080\,320} + \mathcal{O}(\kappa^{10}) \right]. \quad (25)$$

Strictly speaking, it corresponds to an infinite speed of sound in the limit of low frequencies. We note that, because of the logarithmic nature of the singularity, it cannot be observed in Fig. 7.

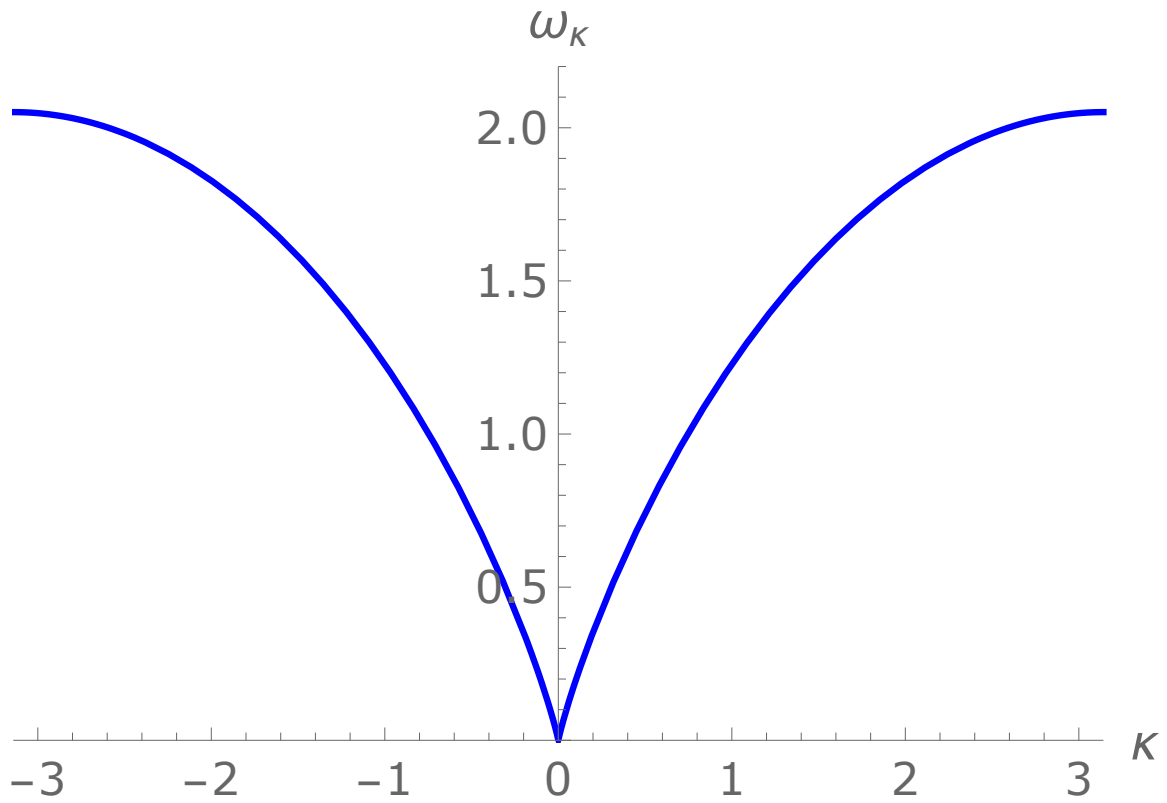


Figure 7: The angular frequency ω_κ of a one-dimensional Wigner crystal as a function of the lattice momentum κ . To put into evidence its behaviour around $\kappa = 0$, we show ω_κ for $\kappa \in [-\pi, \pi]$.

6 Conclusions

In this work, we presented a study of the Thomson problem, in which electrons interact through a repulsive Coulomb interaction, on n -dimensional Clifford Tori \mathcal{T}^n , with $n = 1, 2, 3$. Similarly to what is usually done for the Thomson problem on the surface of the ordinary sphere, \mathcal{S}^2 , the distance that was used in the Coulomb law is the Euclidean distance in the embedding space of the torus, which in this case is the n -dimensional complex space \mathbb{C}^n . We applied our approach to the search of the minimum-energy configurations of Wigner crystals. Our approach permits to simulate a fragment of an infinite Wigner crystal, while avoiding the border effects that are necessarily associated to a finite-cluster calculation within open-boundary conditions. We performed a series of numerical calculations in which we found the minimum Coulomb energy of the system starting from random initial geometries. We showed that, for a sufficiently large number of electrons, the global minima correspond to the linear lattice (1D), the hexagonal lattice (2D) and the body-centred cubic lattice (3D). We cannot exclude, in principle, that other regular structures having lower energies can exist, for instance, by increasing even further the number of electrons. However, our calculations are in agreement with the existing results in the literature on the prediction of the lattice structures of Wigner crystals.

In future works, we plan to generalize the Thomson problem on Clifford tori to different inter-particle potentials. In particular, we will study the behavior of clusters bounded by harmonic potentials. In the limit of systems having a small size with respect to the torus dimension, in fact, the physics of the system should converge to that of the same systems in the ordinary infinite space. In a more general perspective, it will be possible to use completely general distance-dependent particle-particle interactions and replace the ordinary distance in the infinite open space by the Euclidean distance in a toroidal supercell. In this a way, one could perform molecular mechanics simulations on a set of particles, or molecules, in a periodic context. Finally, we will extend our approach to a full quantum treatment of the electrons by extending the approach described in Ref. [20] to more than 2 electrons.

7 Acknowledgements

We thank the French “Agence Nationale de la Recherche (ANR)” for financial support (Grant Agreements No. ANR-19-CE30-0011 and ANR-22-CE29-0001). This work has been (partially) supported through the EUR grant NanoX n° ANR-17-EURE-0009 in the framework of the “Programme des Investissements d’Avenir”.

A The gradient and Hessian of the Coulomb energy

The gradient of the Coulomb energy given in Eq. (2) has the following components

$$\partial_{x_{\alpha,i}} U = -\frac{1}{2} \left(\frac{\pi}{L_{\alpha}} \right) \sum_{\substack{k=1 \\ k \neq i}}^N \left[\sum_{\beta=1}^n \left(\frac{L_{\beta}}{\pi} \right)^2 \sin^2 \left(\frac{\pi}{L_{\beta}} (x_{\beta,i} - x_{\beta,k}) \right) \right]^{-3/2} \sin \left(\frac{2\pi}{L_{\alpha}} (x_{\alpha,i} - x_{\alpha,k}) \right). \quad (26)$$

The Hessian of the Coulomb energy has the following components,

$$\begin{aligned} \partial_{x_{\alpha,i} x_{\alpha,i}}^2 U &= \frac{3}{2} \frac{\pi^2}{L_{\alpha}^2} \sum_{\substack{k=1 \\ k \neq i}}^N \left[\sum_{\beta=1}^n \left(\frac{L_{\beta}}{\pi} \right)^2 \sin^2 \left(\frac{\pi}{L_{\beta}} (x_{\beta,i} - x_{\beta,k}) \right) \right]^{-5/2} \sin^2 \left(\frac{2\pi}{L_{\alpha}} (x_{\alpha,i} - x_{\alpha,k}) \right) \\ &\quad - \sum_{\substack{k=1 \\ k \neq i}}^N \left[\sum_{\beta=1}^n \left(\frac{L_{\beta}}{\pi} \right)^2 \sin^2 \left(\frac{\pi}{L_{\beta}} (x_{\beta,i} - x_{\beta,k}) \right) \right]^{-3/2} \cos \left(\frac{2\pi}{L_{\alpha}} (x_{\alpha,i} - x_{\alpha,k}) \right), \end{aligned} \quad (27)$$

$$\begin{aligned} \partial_{x_{\alpha,i} x_{\alpha,j}}^2 U &= -\frac{3}{2} \left(\frac{\pi}{L_{\alpha}} \right)^2 \sum_{\substack{k=1 \\ k \neq i}}^N \left[\sum_{\beta=1}^n \left(\frac{L_{\beta}}{\pi} \right)^2 \sin^2 \left(\frac{\pi}{L_{\beta}} (x_{\beta,i} - x_{\beta,j}) \right) \right]^{-5/2} \sin^2 \left(\frac{2\pi}{L_{\alpha}} (x_{\alpha,i} - x_{\alpha,j}) \right) \\ &\quad + \sum_{\substack{k=1 \\ k \neq i}}^N \left[\sum_{\beta=1}^n \left(\frac{L_{\beta}}{\pi} \right)^2 \sin^2 \left(\frac{\pi}{L_{\beta}} (x_{\beta,i} - x_{\beta,j}) \right) \right]^{-3/2} \cos \left(\frac{2\pi}{L_{\alpha}} (x_{\alpha,i} - x_{\alpha,j}) \right), \quad (i \neq j) \end{aligned} \quad (28)$$

$$\begin{aligned} \partial_{x_{\alpha,i} x_{\beta,j}}^2 U &= \frac{3}{4} \frac{\pi^2}{L_{\alpha} L_{\beta}} \left[\sum_{\gamma=1}^n \left(\frac{L_{\gamma}}{\pi} \right)^2 \sin^2 \left(\frac{\pi}{L_{\gamma}} (x_{\gamma,i} - x_{\gamma,j}) \right) \right]^{-5/2} \\ &\quad \times \sin \left(\frac{2\pi}{L_{\alpha}} (x_{\alpha,i} - x_{\alpha,j}) \right) \sin \left(\frac{2\pi}{L_{\beta}} (x_{\beta,i} - x_{\beta,j}) \right) \quad (i \neq j, \alpha \neq \beta). \end{aligned} \quad (29)$$

We note that the Hessian matrix can be diagonalized to gain information about the nature of the various stationary points on the energy surface from the eigenvalues and eigenvectors.

References

- (1) Thomson, J. J. On the structure of the atom: an investigation of the stability and periods of oscillation of a number of corpuscles arranged at equal intervals around the circumference of a circle; with the application of the results to the theory of atomic structure. *The London, Edinburgh, and Dublin Philosophical Magazine and Journal of Science* **1904**, 7, 237–265.
- (2) Schwartz, R. E. The five-electron case of Thomson’s problem. *Experimental Mathematics* **2013**, 22, 157–186.
- (3) Rakhmanov, E. A.; Saff, E. B.; Zhou, Y. M. Minimal discrete energy on the sphere. *Math. Res. Lett.* **1994**, 1, 647–662.
- (4) Kuijlaars, A.; Saff, E. Asymptotics for minimal discrete energy on the sphere. *Trans. Am. Math. Soc.* **1998**, 350, 523–538.
- (5) Martínez-Finkelshtein, A.; Maymeskul, V.; Rakhmanov, E. A.; Saff, E. B. Asymptotics for Minimal Discrete Riesz Energy on Curves in \mathbb{R}^d . *Can. J. Math.* **2004**, 56, 529–552.
- (6) Cioslowski, J.; Grzebielucha, E. Parameter-free shell model of spherical Coulomb crystals. *Phys. Rev. E* **2008**, 78, 026416.
- (7) Cioslowski, J. Modified Thomson problem. *Phys. Rev. E* **2009**, 79, 046405.
- (8) Cioslowski, J.; Grzebielucha, E. Zero-point vibrational energies of spherical Coulomb crystals. *J. Chem. Phys.* **2009**, 130, 094902.

- (9) Cioslowski, J. Shell structures of assemblies of equicharged particles subject to radial power-law confining potentials. *J. Chem. Phys.* **2010**, *133*, 234902.
- (10) Cioslowski, J.; Grzebielucha, E. Shell model of assemblies of equicharged particles subject to radial confining potentials. *J. Chem. Phys.* **2011**, *134*, 124305.
- (11) Cioslowski, J.; Albin, J. Shell models of two-dimensional Coulomb crystals: Assessment and comparison with the three-dimensional case. *J. Chem. Phys.* **2012**, *136*, 114306.
- (12) Cioslowski, J.; Albin, J. Electrostatic energy of polygonal charge distributions. *J. Math. Chem.* **2012**, *50*, 1378–1385.
- (13) Cioslowski, J. Note on the asymptotic isomer count of large fullerenes. *J. Math. Chem.* **2014**, *52*, 1–5.
- (14) Cioslowski, J.; Albin, J. Oscillatory and fluctuating terms in energies of assemblies of equicharged particles subject to spherically symmetric power-law confining potentials. *J. Chem. Phys.* **2013**, *139*, 104306.
- (15) Cioslowski, J.; Albin, J. Asymptotic equivalence of the shell-model and local-density descriptions of Coulombic systems confined by radially symmetric potentials in two and three dimensions. *J. Chem. Phys.* **2013**, *139*, 114109.
- (16) Gillespie, R. J.; Nyholm, R. S. Inorganic stereochemistry. *Quarterly Reviews, Chemical Society* **1957**, *11*, 339–380.
- (17) Tavernier, N.; Bendazzoli, G. L.; Brumas, V.; Evangelisti, S.; Berger, J. A. Clifford boundary conditions: A simple direct-sum evaluation of Madelung constants. *The Journal of Physical Chemistry Letters* **2020**, *11*, 7090–7095.
- (18) Tavernier, N.; Bendazzoli, G. L.; Brumas, V.; Evangelisti, S.; Berger, J. A. Clifford boundary conditions for periodic systems: the Madelung constant of cubic crystals in 1, 2 and 3 dimensions. *Theoretical Chemistry Accounts* **2021**, *140*, 106.

- (19) Alves, E.; Bendazzoli, G. L.; Evangelisti, S.; Berger, J. A. Accurate ground-state energies of Wigner crystals from a simple real-space approach. *Physical Review B* **2021**, *103*, 245125.
- (20) Escobar Azor, M.; Alves, E.; Evangelisti, S.; Berger, J. A. Wigner localization in two and three dimensions: An ab initio approach. *J. Chem. Phys.* **2021**, *155*, 124114.
- (21) Wigner, E. On the interaction of electrons in metals. *Physical Review* **1934**, *46*, 1002.
- (22) Wigner, E. Effects of the electron interaction on the energy levels of electrons in metals. *Transactions of the Faraday Society* **1938**, *34*, 678–685.
- (23) Smoleński, T.; Dolgirev, P. E.; Kuhlenkamp, C.; Popert, A.; Shimazaki, Y.; Back, P.; Lu, X.; Kroner, M.; Watanabe, K.; Taniguchi, T.; Esterlis, I.; Demler, E.; Imamoglu, A. Signatures of Wigner crystal of electrons in a monolayer semiconductor. *Nature* **2021**, *595*, 53–57.
- (24) Grimes, C. C.; Adams, G. Evidence for a Liquid-to-Crystal Phase Transition in a Classical, Two-Dimensional Sheet of Electrons. *Phys. Rev. Lett.* **1979**, *42*, 795–798.
- (25) Lozovik, Y.; Yudson, V. Crystallization of a two-dimensional electron gas in a magnetic field. *J. Exp. Theor. Phys. Lett.* **1975**, *22*, 11–12.
- (26) Andrei, E. Y.; Deville, G.; Glattli, D. C.; Williams, F. I. B.; Paris, E.; Etienne, B. Observation of a Magnetically Induced Wigner Solid. *Phys. Rev. Lett.* **1988**, *60*, 2765–2768.
- (27) Goldman, V. J.; Santos, M.; Shayegan, M.; Cunningham, J. E. Evidence for two-dimensional quantum Wigner crystal. *Phys. Rev. Lett.* **1990**, *65*, 2189–2192.
- (28) Williams, F. I. B.; Wright, P. A.; Clark, R. G.; Andrei, E. Y.; Deville, G.; Glattli, D. C.; Probst, O.; Etienne, B.; Dorin, C.; Foxon, C. T.; Harris, J. J. Conduction threshold

- and pinning frequency of magnetically induced Wigner solid. *Phys. Rev. Lett.* **1991**, *66*, 3285–3288.
- (29) Ye, P. D.; Engel, L. W.; Tsui, D. C.; Lewis, R. M.; Pfeiffer, L. N.; West, K. Correlation Lengths of the Wigner-Crystal Order in a Two-Dimensional Electron System at High Magnetic Fields. *Phys. Rev. Lett.* **2002**, *89*, 176802.
- (30) Chen, Y. P.; Sambandamurthy, G.; Wang, Z. H.; Lewis, R. M.; Engel, L. W.; Tsui, D. C.; Ye, P. D.; Pfeiffer, L. N.; West, K. W. Melting of a 2D quantum electron solid in high magnetic field. *Nat. Phys.* **2006**, *2*, 452–455.
- (31) Jang, J.; Hunt, B. M.; Pfeiffer, L. N.; West, K. W.; Ashoori, R. C. Sharp tunnelling resonance from the vibrations of an electronic Wigner crystal. *Nat. Phys.* **2017**, *13*, 340–344.
- (32) Regan, E. C.; Wang, D.; Jin, C.; Bakti Utama, M. I.; Gao, B.; Wei, X.; Zhao, S.; Zhao, W.; Zhang, Z.; Yumigeta, K.; Blei, M.; Carlström, J. D.; Watanabe, K.; Taniguchi, T.; Tongay, S.; Crommie, M.; Zettl, A.; Wang, F. Mott and generalized Wigner crystal states in WSe₂/WS₂ Moiré superlattices. *Nature* **2020**, *579*, 359–363.
- (33) Tang, Y.; Li, L.; Li, T.; Xu, Y.; Liu, S.; Barmak, K.; Watanabe, K.; Taniguchi, T.; MacDonald, A. H.; Shan, J.; Mak, K. F. Simulation of Hubbard model physics in WSe₂/WS₂ Moiré superlattices. *Nature* **2020**, *579*, 353–358.
- (34) Xu, Y.; Liu, S.; Rhodes, D. A.; Watanabe, K.; Taniguchi, T.; Hone, J.; Elser, V.; Mak, K. F.; Shan, J. Correlated insulating states at fractional fillings of Moiré superlattices. *Nature* **2020**, *587*, 214–218.
- (35) Li, H.; Li, S.; Regan, E. C.; Wang, D.; Zhao, W.; Kahn, S.; Yumigeta, K.; Blei, M.; Taniguchi, T.; Watanabe, K.; Tongay, S.; Zettl, A.; Crommie, M. F.; Wang, F. Imaging two-dimensional generalized Wigner crystals. *Nature* **2021**, *597*, 650–654.

- (36) Deshpande, V. V.; Bockrath, M. The one-dimensional Wigner crystal in carbon nanotubes. *Nat. Phys.* **2008**, *4*, 314–318.
- (37) Shapir, I.; Hamo, A.; Pecker, S.; Moca, C. P.; Legeza, Ö.; Zarand, G.; Ilani, S. Imaging the electronic Wigner crystal in one dimension. *Science* **2019**, *364*, 870–875.
- (38) Ziani, N. T.; Cavaliere, F.; Becerra, K. G.; Sasseti, M. A Short Review of One-Dimensional Wigner Crystallization. *Crystals* **2021**, *11*, 20.
- (39) Cioslowski, J.; Buchowiecki, M. Wigner molecules: Natural orbitals of strongly correlated two-electron harmonium. *J. Chem. Phys.* **2006**, *125*, 064105.
- (40) Ellenberger, C.; Ihn, T.; Yannouleas, C.; Landman, U.; Ensslin, K.; Driscoll, D.; Gosard, A. C. Excitation Spectrum of Two Correlated Electrons in a Lateral Quantum Dot with Negligible Zeeman Splitting. *Phys. Rev. Lett.* **2006**, *96*, 126806.
- (41) Yannouleas, C.; Landman, U. Symmetry breaking and quantum correlations in finite systems: studies of quantum dots and ultracold Bose gases and related nuclear and chemical methods. *Rep. Prog. Phys.* **2007**, *70*, 2067–2148.
- (42) Mendl, C. B.; Malet, F.; Gori-Giorgi, P. Wigner localization in quantum dots from Kohn-Sham density functional theory without symmetry breaking. *Phys. Rev. B* **2014**, *89*, 125106.
- (43) Cioslowski, J. One-electron densities of freely rotating Wigner molecules. *J. Phys. B: At. Mol. Opt. Phys.* **2017**, *50*, 235102.
- (44) Cioslowski, J.; Strasburger, K. Harmonium atoms at weak confinements: The formation of the Wigner molecules. *J. Chem. Phys.* **2017**, *146*, 044308.
- (45) Egger, R.; Häusler, W.; Mak, C. H.; Grabert, H. Crossover from Fermi Liquid to Wigner Molecule Behavior in Quantum Dots. *Phys. Rev. Lett.* **1999**, *82*, 3320–3323.

- (46) Diaz-Marquez, A.; Battaglia, S.; Bendazzoli, G. L.; Evangelisti, S.; Leininger, T.; Berger, J. A. Signatures of Wigner localization in one-dimensional systems. *J. Chem. Phys.* **2018**, *148*, 124103.
- (47) Telleria-Alлика, X.; Escobar Azor, M.; François, G.; Bendazzoli, G. L.; Matxain, J. M.; Lopez, X.; Evangelisti, S.; Berger, J. A. The Wigner localization of interacting electrons in a one-dimensional harmonic potential. *J. Chem. Phys.* **2022**, *157*, 174107.
- (48) Escobar Azor, M.; Brooke, L.; Evangelisti, S.; Leininger, T.; Loos, P.-F.; Suaud, N.; Berger, J. A. A Wigner molecule at extremely low densities: a numerically exact study. *SciPost Phys. Core* **2019**, *1*, 001.
- (49) Pecker, S.; Kuemmeth, F.; Secchi, A.; Rontani, M.; Ralph, D. C.; McEuen, P. L.; Ilani, S. Observation and spectroscopy of a two-electron Wigner molecule in an ultra-clean carbon nanotube. *Nat. Phys.* **2013**, *9*, 576–581.
- (50) Méndez-Camacho, R.; Cruz-Hernández, E. Asymmetric Wigner molecules in nanowire Y-junctions. *Scientific Reports* **2022**, *12*, 20183.
- (51) Méndez-Camacho, R.; Cruz-Hernández, E. Tunneling between parallel one-dimensional Wigner crystals. *Scientific Reports* **2022**, *12*, 4470.
- (52) Thakur, T.; Szafran, B. Wigner molecules in phosphorene quantum dots. *Phys. Rev. B* **2022**, *106*, 205304.
- (53) Valença Ferreira de Aragão, E.; Moreno, D.; Battaglia, S.; Bendazzoli, G. L.; Evangelisti, S.; Leininger, T.; Suaud, N.; Berger, J. A. A simple position operator for periodic systems. *Phys. Rev. B* **2019**, *99*, 205144.
- (54) Sholl, C. A. The calculation of electrostatic energies of metals by plane-wise summation. *Proc. Phys. Soc.* **1967**, *92*, 434.

- (55) Hasse, R.; Avilov, V. V. Structure and Madelung energy of spherical Coulomb crystals.
Phys. Rev. A **1991**, *44*, 4506.
- (56) <https://github.com/ALRAKIK/Thomson> (accessed 11 August 2023).

TOC Graphic

